


 Cite this: *Lab Chip*, 2026, 26, 2368

Intensified lentiviral vector perfusion bioprocessing with a spiral inertial microfluidic cell retention device

 Alexander Bevacqua, ^{abc} Fuguo Liu,^{cd} Jianzhu Chen^{ce} and Jongyoon Han ^{*abf}

Scalable production of cell therapy doses relies on inexpensive, efficient production of gene delivery vectors, such as lentiviral vectors, in HEK293 cell culture. Intensified perfusion processes improve the volumetric productivity of cell culture by continuously supplying nutrients, oxygen, and media to cells while removing harmful metabolites, thereby enabling higher producer cell densities. Membrane filter-based cell retention devices commonly used in perfusion bioprocessing can experience significant clogging and fouling over long-term processes, which leads to the undesired retention of lentiviral vectors in the filter matrix. In this work, we used spiral microfluidic technology as a cell retention device to continuously harvest lentiviral vectors and remove metabolic waste from HEK293 cells in a bioreactor running high cell density perfusion cultures. With the spiral microfluidic device, we performed four perfusion culture runs with maximum cell densities between 15×10^6 and 25×10^6 cells per mL, achieving up to seven days of continuous lentiviral vector production and lossless harvesting with maximum, unconcentrated, functional titers on the order of 10^8 transducing units (TU) per mL. These production titers are competitive with other bioprocessing approaches in industry and academia. The highest cell-specific productivity (over 50 TU per cell per day) and cell-specific yields of our study (over 80 TU per cell) were achieved when using spiral device-mediated perfusion bioprocessing to cultivate cells and then transferring the cells to a shake flask environment with daily media replacement to generate lentiviral vectors.

 Received 11th January 2026,
 Accepted 9th March 2026

DOI: 10.1039/d6lc00029k

rsc.li/loc

1. Introduction

Lentiviral vectors (LVs) are engineered retroviruses capable of efficiently delivering a gene of interest, or transgene, into target cells. They are valuable tools for the development and large-scale manufacturing of cell therapies, offering efficient and stable gene delivery of a transgene to the host genomes of dividing and non-dividing cells.¹ LVs have been used to design cell therapy formulations across both *in vivo* and *ex vivo* therapeutic modalities, targeting lung, brain, and eye tissues in the former, and targeting T cells, natural killer

cells, and stem cells in the latter.² Clinical applications of cell therapies and lentiviral vectors are growing, as evidenced by the rising number of clinical trials involving LV-based formulations, and their long-term success will depend on the reliable, high-titer production of LVs.²

Depending on the tissue target and modality, the LV dose can range from 10^6 to 10^{11} transducing units (TU) of functional virus particles.² For Chimeric Antigen Receptor (CAR)-T *ex vivo* therapies, the dose size is on the order of 10^9 TU.^{2,3} Typical production functional titers range from 10^6 to 10^8 TU mL⁻¹, with cell-specific productivities generally lower than 10 TU per cell per day, depending on the production strategy. To achieve higher titers and cell-specific productivities, optimizing the upstream process and LV harvest is necessary. This includes cell line selection, plasmid design, transfection strategy, culture media formulation, and bioreactor operation. Innovations, including suspension cell lines,⁴ stable producer cell lines,⁴ and intensified perfusion processes,^{5,6} have led to high production titers and, in turn, lower production costs.^{2,5}

Suspension-adapted cell lines can be cultured in stirred-tank bioreactors and can be scaled to hundreds of liters, whereas adherent cell lines have limited scalability.² While lentiviral vectors are conventionally produced by transient transfection of plasmid DNA, stable producer cell lines possess all of the

^a Department of Biological Engineering, Massachusetts Institute of Technology, Cambridge, Massachusetts, USA. E-mail: jyhan@mit.edu

^b Research Laboratory of Electronics, Massachusetts Institute of Technology, Cambridge, Massachusetts, USA

^c Koch Institute for Integrative Cancer Research, Massachusetts Institute of Technology, Cambridge, Massachusetts, USA

^d Dana-Farber Cancer Institute, Harvard Medical School, Boston, Massachusetts, USA

^e Department of Biology, Massachusetts Institute of Technology, Cambridge, Massachusetts, USA

^f Department of Electrical Engineering and Computer Science, Massachusetts Institute of Technology, Cambridge, Massachusetts, USA



components needed for LV production, and its trigger is often controlled by an inducible gene switch.^{4,7} In addition to eliminating the need to generate large quantities of transfection-grade plasmid DNA for transient transfection, the production titers with stable producer cell lines have lower batch-to-batch variability than those produced by transient transfection.⁸ Suspension-adapted stable producer cells can be cultivated in stirred-tank bioreactors with intensified perfusion bioprocessing to achieve higher cell densities and increase cell-specific productivity. To accomplish this, a cell retention device is used to simultaneously remove waste and harvest products as they are generated, while retaining cells in the bioreactor. The continuous harvesting of viral vectors from culture and storage at 4 °C is particularly advantageous because LVs are fragile to pH, salt concentration, and shear stress, with an approximate half-life of 3 to 18 hours at 37 °C.^{6,9}

Hollow fiber filter-based systems, currently used as cell retention devices for perfusion culture, include tangential flow filtration (TFF), alternating tangential flow (ATF) filtration, and tangential flow depth filtration (TFDF). These cell retention devices, however, are challenging to use for viral vector harvesting due to membrane fouling and the undesired retention of dead cells and products in the filter over long production periods and harvests.^{6,10} These drawbacks lead to increases in transmembrane pressure across the filter over time.^{3,5} One of the most significant bottlenecks in vector manufacturing is the loss during recovery from host cell culture supernatant, with vector recoveries ranging from 30% to 80% depending on the downstream processing strategies involved.¹¹ Despite these challenges, filtration-based cell retention devices are commercially mature, with a wide range of products tailored for various bioreactor scales.⁵ Consequently, they represent the current industry standard in existing biomanufacturing workflows.

Spiral microfluidic technology is a label-free, membraneless, and continuous particle-separation strategy that has previously been used as a cell retention device in perfusion culture and for the clarification of Chinese hamster ovary (CHO) cells for antibody production.^{10,12–14} Clogging is virtually impossible with this device, since the channel sizes are much larger than the cells. The spiral cell retention device also has the unique ability to avoid membrane fouling and separate dead cells and

cell aggregates from the main culture.¹⁵ When adapted to lentiviral vector perfusion bioprocessing in Fig. 1, the spiral microfluidic device receives cell culture fluid into the inlet at the spiral's center. Human embryonic kidney 293 (HEK293) cells (~18 to 21 μm in diameter) travel along the spiral and are hydrodynamically focused along the spiral's inner wall to the inward outlet, while the LVs (~80 to 120 nm in diameter)¹⁶ are randomly dispersed and relatively unaffected by inertial focusing, so they can be harvested through the outward outlet.

In this study, we integrated spiral microfluidic technology with a conventional bioreactor setup for lentiviral vector perfusion bioprocessing. We produced LVs from a suspension-adapted, inducible, HEK293 stable lentiviral vector producer cell line in perfusion culture and used spiral microfluidic cell retention technology to remove metabolic waste, cultivate cells, and harvest LVs from the main culture vessel. Since the spiral microfluidic device offers a membraneless option that does not clog, experience fouling, or lose significant amounts of product to matrix entrapment, the titers we achieve with the device are competitive with other benchmarks, making spiral microfluidics a feasible option for LV intensification at various volume scales.

2. Experimental methods

2.1 Media formulations

There are two medium formulations primarily used during the bioprocessing runs. Non-inducing medium is used before the lentiviral vector production phase and refers to Hycell-Transfx-H (Cytiva) supplemented with 4 mM L-glutamine, surfactant Kolliphor P188 0.1% v/v media (Sigma-Aldrich, USA), and 1% v/v penicillin-streptomycin (Thermo Fisher Scientific, USA). During the lentiviral vector production phase, inducing medium is perfused to the bioreactor, which is Hycell-Transfx-H (Cytiva) supplemented with 4 mM L-glutamine, surfactant Kolliphor P188 0.1% v/v media (Sigma-Aldrich, USA), 1% v/v penicillin-streptomycin (Thermo Fisher Scientific, USA), 110 μg mL⁻¹ cumate (Sigma-Aldrich, USA), and 12 nM coumermycin A1 (Santa Cruz Biotechnology, USA). One day post-induction, 7 mM of sodium butyrate (Sigma Aldrich, USA) is also added into the inducing medium.

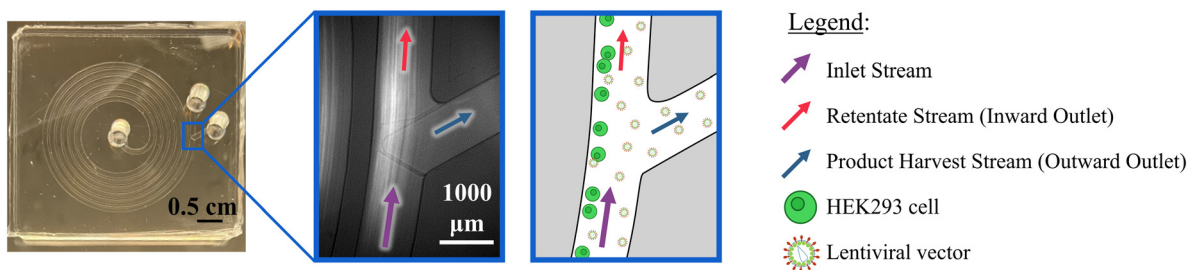


Fig. 1 A picture of a polydimethylsiloxane (PDMS) spiral microfluidic cell retention device used to maintain perfusion cultures of HEK293 cells. The inlet stream originates from the center of the spiral, and the separation junction divides incoming flow into the retentate stream (inward outlet of the spiral) and the product harvest stream (outward outlet of the spiral).



2.2 Cell culture

A HEK293 producer clone engineered to generate LV-CMV-GFP lentiviral vectors following the addition of cumate and coumermycin (a gift from Dr. Aziza P. Manceur of the National Research Council Canada) was thawed from storage in liquid nitrogen and centrifuged at 300g for 5 minutes at room temperature. The supernatant is discarded, and the cells are resuspended in non-inducing media. The cells are cultured in non-inducing media in 125 mL to 500 mL shake flasks at 37 °C in a 5% CO₂ atmosphere at 135 rotations per minute (rpm) on an orbital shaker (19 mm orbit) until they are used for inoculation in the bioreactor. Once the cell density in the bioreactor exceeded the target cell density in a run, a 10 mL solution of cumate and coumermycin in non-inducing media was added to the bioreactor to raise the concentration of inducer molecules in the bioreactor to 110 μg mL⁻¹ cumate and 12 nM coumermycin instantaneously. Immediately after adding this 10 mL solution, the media feed was switched to inducing media for the days to follow. One day post-induction, sodium butyrate was added to the bioreactor to a final concentration of 7 mM and maintained at this concentration for the remaining duration of the experiment. LV titer improves when supplemented with sodium butyrate one day post-induction.^{7,17–19} It is hypothesized that this titer enhancement occurs because sodium butyrate acts as a histone deacetylase inhibitor, facilitating transcription and leading to higher expression of Gag, Rev, and VSV-G.⁷

2.3 Spiral microfluidic device preparation

The PDMS spiral cell retention device, illustrated in Fig. 1, is prepared using a 10:1 volume mixture of PDMS to Sylgard 184 (curing agent) in a negative mold of the device.¹⁰ The mixture is degassed in a vacuum chamber for up to 30 minutes. Curing is done for 2 hours at 65 °C. A biopsy punch tool with a 4 mm diameter is used to create the inlet and outlet holes in the device. A 1 minute plasma treatment is used to bond the PDMS slab to a glass slide. Curing is done for 2 to 6 hours at 65 °C, and then the device is ready to use.

2.4 Bioreactor preparation and batch mode

The perfusion culture assembly is illustrated in Fig. 2(a). Briefly, an Applikon MiniBio 500 bioreactor controlled using the Applikon my-Control bioreactor system is connected to a harvest bottle, a medium bottle (with either non-inducing media or inducing media depending on the stage of the culture), the spiral microfluidic device, a bottle containing Antifoam C Emulsion (Sigma Aldrich, USA) in DI water, and a bottle with sodium bicarbonate base (for pH control), all using Masterflex tubing (L/S 13, L/S 14, and L/S 16 sizes). Three peristaltic pumps are used to control the spiral microfluidic device's input flow rate Q_{inlet} , the spiral microfluidic device's harvest flow rate Q_{harvest} , and the cell culture medium flow rate Q_{media} . Gas cylinders with air, O₂, and CO₂ are attached to the Applikon my-Control bioreactor system. The bioreactor's sensors, such as the pH and dO₂

sensors, are then calibrated. The entire assembly, excluding the peristaltic pumps, is then autoclaved as a closed system in a gravity sterilization cycle. The bioreactor is inoculated at a target viable cell density of 0.35×10^6 (0.35 million per mL, M mL⁻¹). The stirring rate, pH, dissolved oxygen percentage (dO₂), and temperature are controlled and recorded *via* the Applikon my-Control system and the Lucullus PIMS software, respectively. The starting setpoint values are 500 rpm stirring rate, pH 7.1, 60% dO₂, and 37 °C. The stirring rate is increased in increments of 50 rpm to minimize cell aggregation, within a range of 500 to 700 rpm. The three primary sample sources of the perfusion culture are illustrated in Fig. 2(a): bioreactor, harvest line, and harvest bottle. A photograph of part of the perfusion culture setup is shown in Fig. 2(b) to illustrate the connection between the bioreactor and the spiral device and to compare their sizes.

2.5 Perfusion mode

Three days after inoculation, perfusion mode begins by operating the three peristaltic pumps (Fig. 2(a)). Q_{inlet} is set to 6 mL min⁻¹ for the cell retention device, since it must be sufficiently fast to maintain proper inertial focusing of cells into the retentate stream, but slow enough to avoid significantly reducing cell viability.

The perfusion rate, measured in vessel volumes per day (VVD), was adjusted throughout the run from 0.5 to 1 VVD.

$$\text{VVD} = \frac{Q_{\text{media}}}{V_{\text{vessel}}}$$

where Q_{media} is the volumetric flow rate of media added to the bioreactor, which is equal to the volumetric flow rate harvested from the bioreactor, written on a 'per day' basis, and V_{vessel} is the working volume of the bioreactor (for the Applikon MiniBio 500, we use 350 mL).

The cell-specific perfusion rate (CSPR) is the perfusion rate divided by the viable cell density in the bioreactor.

$$\text{CSPR} = \frac{\text{VVD}}{\text{VCD}_{\text{Bioreactor}}}$$

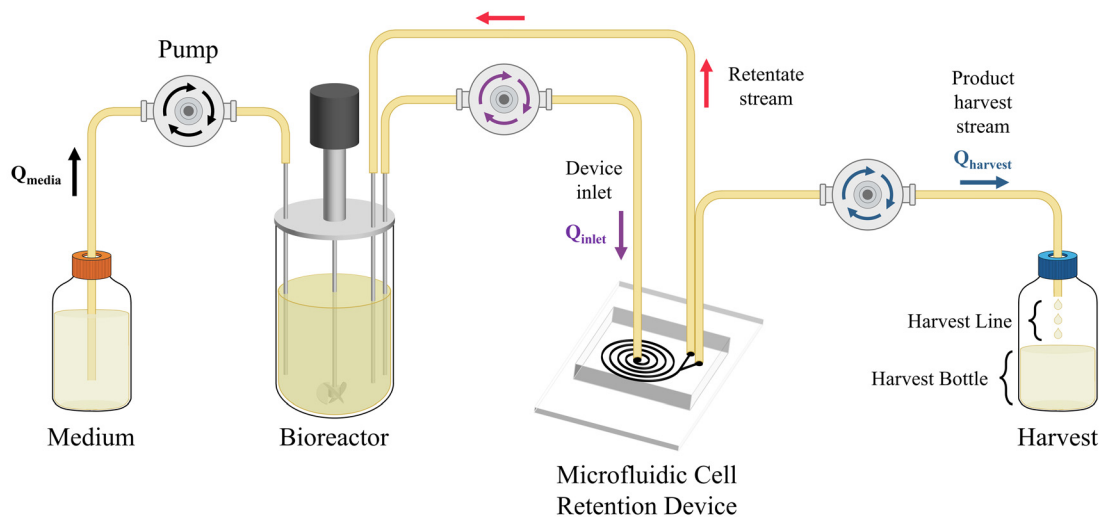
where VVD is the perfusion rate and $\text{VCD}_{\text{Bioreactor}}$ is the viable cell density in the bioreactor.

The VVD was progressively increased over the course of the cell growth phase, while accounting for the cell densities and metabolite concentrations measured daily with the FLEX2 Cell Culture Analyzer (Nova Biomedical, USA), an appropriate CSPR, and an effective spiral device harvest flow rate. The harvest flow rate (Q_{harvest}) is proportional to the VVD. Therefore, the harvest ratio $\left(\frac{Q_{\text{harvest}}}{Q_{\text{inlet}}}\right)$, which is usually set to 1/15 or lower for spiral microfluidic technology to maintain high cell focusing performance, depends on the Q_{inlet} and the VVD.

Each day, cell density measurements are recorded from the bioreactor and the harvest bottle. The harvest bottle is replaced daily. Once lentiviral vector production is onset, the perfusion rate is set to 1 VVD (0.24 mL min⁻¹) across all experiments for



(a)



(b)

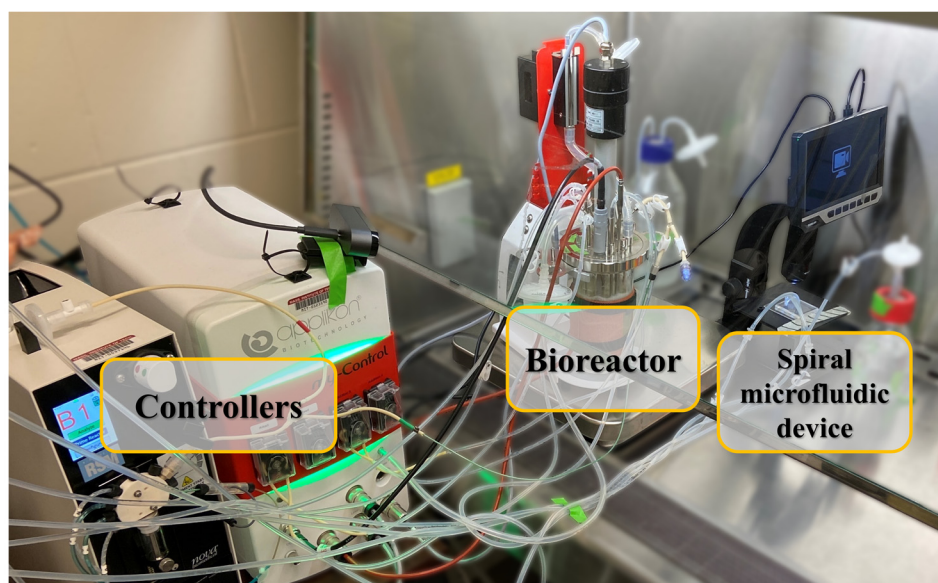


Fig. 2 (a) A simplified schematic illustrating the perfusion culture assembly with the spiral microfluidic cell retention device in an external loop connected to the bioreactor. Cell culture fluid is continuously pumped into the microfluidic cell retention device and split into two streams. The product harvest stream is downstream of the outward outlet of the spiral device, which contains a cell-free viral vector solution that accumulates in the harvest (at 4 °C). Harvest line samples are instantaneous samples taken from the liquid drops that are currently falling into the bottle. Harvest bottle samples are time-averaged samples of the liquid accumulating over the previous 24 hours. The retentate stream is downstream of the inward outlet of the spiral device, and it contains HEK293 cells and viral vectors. The volumetric flow rates of the peristaltic pumps are as follows: $Q_{\text{inlet}} = 6 \text{ mL min}^{-1}$ and $Q_{\text{media}} = Q_{\text{harvest}} = 0.12 \text{ to } 0.24 \text{ mL min}^{-1}$, depending on the perfusion rate. (b) A photograph of the perfusion culture assembly with the spiral microfluidic device acting as a cell retention device.

each day of LV harvest. Cell density measurements are taken from the bioreactor, harvest line, and harvest bottle from that point onward.

2.6 Post-induction perfusion bioreactor and pseudo-perfused shake flask

In perfusion culture runs 1 and 2, once the total cell density exceeded 15 M mL^{-1} , half of the bioreactor volume (175 mL

of cells) was transferred to a glass shake flask (referred to as the pseudo-perfused shake flask), and the remaining 175 mL of cells stayed in the bioreactor. Both the perfusion bioreactor and the shake flask were filled back to 350 mL with a final concentration of $110 \mu\text{g mL}^{-1}$ cumate and 12 nM coumermycin. Once the dilution and induction are complete, the perfusion bioreactor is operated continuously at 1 VVD (with inducing media) and the pseudo-perfused shake flask was resuspended once daily with inducing media (effectively



operating at 1 VVD). The pseudo-perfused shake flask was maintained at 37 °C in a 5% CO₂ atmosphere and agitated at 135 rpm with an orbital shaker (19 mm orbit). Sodium butyrate treatment in both vessels was the same as described above. Consequently, the perfusion bioreactor and pseudo-perfused shake flask are now set up to originate from the same high-VCD, spiral device-mediated cell population, undergo the same induction strategy, have an equal working volume, and experience the same perfusion rate of 1 VVD. LV generation in the perfusion bioreactor facilitates a continuous harvest of product into the refrigerated harvest bottle and a lower average residence time of LVs at 37 °C, which may lead to lower rates of thermal degradation compared to the daily batch exchange of the pseudo-perfused shake flask. This advantage is balanced by the intermittent exposure of cells to elevated shear stresses needed for spiral microfluidic cell retention, which is absent in the pseudo-perfused shake flask condition.

2.7 Lentiviral vector collection and functional titer measurements

Following induction of the perfusion bioreactor (and pseudo-perfused shake flask, if applicable), samples are withdrawn from the bioreactor, harvest line, harvest bottle, and pseudo-perfused shake flask. Generally, the bioreactor and pseudo-perfused shake flask had far higher cell densities than the harvest line and harvest bottle samples, but for operational consistency, all samples were centrifuged at 300g for 5 minutes and filtered through a 0.45 μm surfactant-free cellulose acetate (SFCA) filter (Corning, USA). These lentiviral vector samples were stored at -80 °C.

Jurkat cells were cultured at 37 °C in a 5% CO₂ atmosphere in Gibco Roswell Park Memorial Institute (RPMI) 1640 Medium (Thermo Fisher, USA). RPMI 1640 was supplemented with 10% v/v fetal bovine serum (FBS), 2 mM L-glutamine, and 1% v/v penicillin–streptomycin. Jurkat cells (0.5 × 10⁶ viable cells in a 500 μL volume) were transduced in 24-well plates in the presence of 10 μg mL⁻¹ polybrene and centrifuged at 1000g for 1 hour at 37 °C. The plates are then transferred to an incubator held at 5% CO₂ and 37 °C. 24 hours post-transduction, 500 μL of fresh RPMI 1640 supplemented with 10% v/v FBS, 2 mM L-glutamine, and 1% v/v penicillin–streptomycin is added to each well. 60 hours post-transduction, the cells were resuspended in phosphate-buffered saline (PBS) containing 1% bovine serum albumin (BSA) and DAPI for live/dead staining. Data were acquired on the FACSymphony A3 flow cytometer (BD Biosciences, USA) with FACSDiva software, where GFP expression was detected with the BB515 channel, and DAPI fluorescence was collected with the BV421 channel.

Untransduced Jurkat cells, heat-killed untransduced Jurkat cells, and an LV standard are included in the assay as controls used for the gating strategy. Heat-killing of cells for their respective controls is done on a heat block set to 70 °C for 10 minutes. Further analysis was done using FlowJo v10 (BD Biosciences, USA). Live single cells were gated based on

forward scatter, side scatter, and DAPI, and GFP+ cells were quantified within this population. Details on the gating strategy are shown in Fig. S1. A Poisson distribution is used to describe the relationship between GFP+ percentage and multiplicity of infection (MOI) (shown in Fig. S2) and to calculate the functional titer.²⁰ More details on the calculations are available in the SI.

2.8 Measuring spiral device performance

The device's performance is evaluated quantitatively with two metrics: the cell retention efficiency, which measures how adequately the spiral microfluidic device is sorting cells to the retentate stream (inward outlet), and the titer ratio, which is the quotient of the product titer in the harvest stream (outward outlet) and the product titer in the device's feed stream or the bioreactor.¹⁰

Cell retention efficiency on day *i* is defined as:

$$\text{CRE}_i = 100\% - \frac{\text{TCD}_{\text{Harvest Bottle},i}}{\text{TCD}_{\text{Bioreactor},i}}$$

where TCD_{Harvest Bottle,*i*} is the total cell density in the harvest bottle on day *i* and TCD_{Bioreactor,*i*} is the total cell density in the bioreactor on day *i*.

Titer ratio on day *i* is defined as:

$$\text{TR}_i = \frac{\text{titer}_{\text{Harvest Line},i}}{\text{titer}_{\text{Bioreactor},i}}$$

where titer_{Harvest Line,*i*} is the functional titer in the harvest line on day *i* and titer_{Bioreactor,*i*} is the functional titer in the bioreactor on day *i*.

2.9 Cell-specific LV productivity and yield

Equations for cell-specific productivity and cell-specific yield are adapted from the works of Coronel *et al.*²¹ and Klimpel *et al.*,⁵ with simplifying assumptions. Since all vector harvests are done at 1 VVD and measurements are done daily, the formula used by Klimpel *et al.* for cell-specific productivity on day *i* of perfusion culture can be streamlined to:

$$q_{\text{LV},i} \cong \frac{(\text{titer}_{\text{Bioreactor},i} - \text{titer}_{\text{Bioreactor},i-1}) + \text{titer}_{\text{Harvest Bottle},i}}{\frac{1}{2}(\text{VCD}_{\text{Bioreactor},i} + \text{VCD}_{\text{Bioreactor},i-1})}$$

where $q_{\text{LV},i}$ is the cell-specific productivity (TU per cell per day) on day *i*, titer_{Bioreactor,*i*} is the functional titer in the bioreactor on day *i*, titer_{Bioreactor,*i*-1} is the functional titer in the bioreactor on day *i* - 1, titer_{Harvest Bottle,*i*} is the functional titer in the harvest bottle on day *i*, VCD_{Bioreactor,*i*} is the viable cell density in the bioreactor on day *i*, and VCD_{Bioreactor,*i*-1} is the viable cell density in the bioreactor on day *i* - 1.

Cell-specific productivity is estimated based on the process parameters between one day and the next. Since LVs are known to degrade within 24 hours at 37 °C,⁵ there is a relatively short time window during which the LVs can be harvested and stored at 4 °C.



Cell-specific yield estimates the total vector yield produced and harvested per cell:

$$Q_{LV,i} \cong \sum_{j=\text{ind}_D}^i q_{LV,j}$$

where $Q_{LV,i}$ is the cell-specific yield (TU per cell) up until and including day i , $q_{LV,j}$ is the cell-specific productivity (TU per cell per day) on day j , and ind_D is the day of induction.

2.10 Computational fluid dynamics modeling and hydrodynamic regime

Fluid flow and inertial focusing simulations were performed in version 6.3 of COMSOL Multiphysics. These models were used to describe the hydrodynamic conditions experienced by producer cells as they travelled through the device. 0.5 VVD conditions were simulated (6 mL min⁻¹ inlet flow rate and 0.12 mL min⁻¹ harvest flow rate). The hydrodynamic regime of the spiral device, the perfusion bioreactor, and the pseudo-perfused shake flask are quantified using the Reynolds number. Specific calculations are available in the SI. The equation for Reynolds number in a bioreactor and a shake flask is adapted from the work of Dinter *et al.*²²

3. Results and discussion

3.1 Enabling high cell density perfusion cultures

We present results from one of the four perfusion culture runs using the spiral microfluidic cell retention device in Fig. 3. The other three supporting runs are summarized in Fig. S3–S5. In Fig. 3(a), we present time-series data of the total cell density and cell retention efficiency of the bioreactor vessel during a perfusion culture. Each perfusion culture run is characterized by an upward trend in cell density, called the cell growth phase, followed by a downward trend in cell density during the lentiviral vector production phase. Generally, cell density rises initially post-induction, but a prolonged decline begins within two days post-induction (dpi) as the cells commit to vector generation. In run 1 (Fig. 3(a)), the cell density in the bioreactor reached 17.9 M mL⁻¹ with log-phase cell growth. Half of the bioreactor's volume was transferred to a shake flask (referred to as the pseudo-perfused shake flask), and both vessels were induced to generate LVs at the same time (Fig. 3(b)), which were each perfused at 1 VVD. We report a similar outcome in run 2 (reaching 18.0 M mL⁻¹; Fig. S3(a)), in which production was split between the perfusion bioreactor and the pseudo-perfused shake flask to compare their LV outputs. Runs 3 and 4 (Fig. S4 and S5) did not have pseudo-perfused shake flask conditions, and their bioreactors had peak cell densities of 15.3 M mL⁻¹ and 25.3 M mL⁻¹, respectively.

The cell retention efficiency of the spiral microfluidic device throughout the process is typically 96 to 99% (Fig. 3(a)), but on days when the cell density in the bioreactor is high (over 20 M mL⁻¹, see run 4 in Fig. S5(a)) or there is significant dead cell clumping seen in the channels (from lentiviral vector

production) which would disrupt the inertial focusing, the cell retention efficiency can be lower. In Table 1, the spiral cell retention device's mean retention efficiency and the lowest one-day retention efficiency are reported. The cell densities measured in the harvest bottle and harvest line were negligible when compared with the cell densities in the perfusion bioreactor. Fig. S6 compares the cell densities of all sample sources (bioreactor, harvest line, harvest bottle, and pseudo-perfused shake flask if applicable).

To support our experimental cell retention results, flow through the spiral device was studied with a computational fluid dynamics (CFD) model. The maximum simulated fluid velocity in the channel was 1.2 m s⁻¹ and the pressure difference from the device inlet to the outlet was 110 kPa. Spatial profiles of velocity and pressure are presented in Fig. S7(a) and (b). The flow was characterized as within the laminar regime, with a Reynolds number of 245.1 and a Dean number of 24.7 to 37.1 (details in the SI), suggesting a controlled inertial focusing of cell-sized particles towards the inward outlet. A particle-tracing simulation of 150 cell-sized particles (20 μm in diameter) through the device was performed to substantiate this and it shows all particles inertially focusing near the inner wall of the spiral and exiting through the retentate stream (Fig. S7(c)). The Dean vortices that contribute to the inertial focusing of cells are presented in Fig. S7(d) and (e).

3.2 High-titer production of lentiviral vectors

Once lentiviral vector production is initiated with the addition of cumate and coumermycin, samples are withdrawn from the bioreactor, the harvest line, and the harvest bottle. Additionally, in runs 1 and 2, samples are withdrawn from the pseudo-perfused shake flask. The functional titers reported between 1 and 5 days post-induction for run 1 are shown in Fig. 3(b). The highest functional titers were observed 2 to 3 days post-induction for all four runs. The pseudo-perfused shake flask had the highest titer of all the sample sources in runs 1 and 2 (Fig. 3(b) and S3(b)). This suggests that the shear stress imposed on cells by the spiral device may be disadvantageous for lentiviral vector production, and that it is best to pursue only the cell growth phase with the spiral microfluidic cell retention device. Cell clarification could then be performed with the same spiral device. Nevertheless, the maximum functional titers achieved in the perfusion bioreactor, on the order of 10⁷ to 10⁸ TU mL⁻¹ with the spiral cell retention device, are still competitive with the state of the art (see Table 3). Run 4, despite having the highest cell density, had the lowest functional titer (Fig. S5(b)). This was likely due to the cell density plateauing and entering the stationary phase. It would have been more advantageous to begin lentiviral vector production during log-phase growth, as observed in runs 1, 2, and 3.

The onset of perfusion mode with the spiral device and the onset of lentiviral vector production led to observable changes in the bioreactor's process parameters. For instance, the concentration of nutrients and metabolites in the



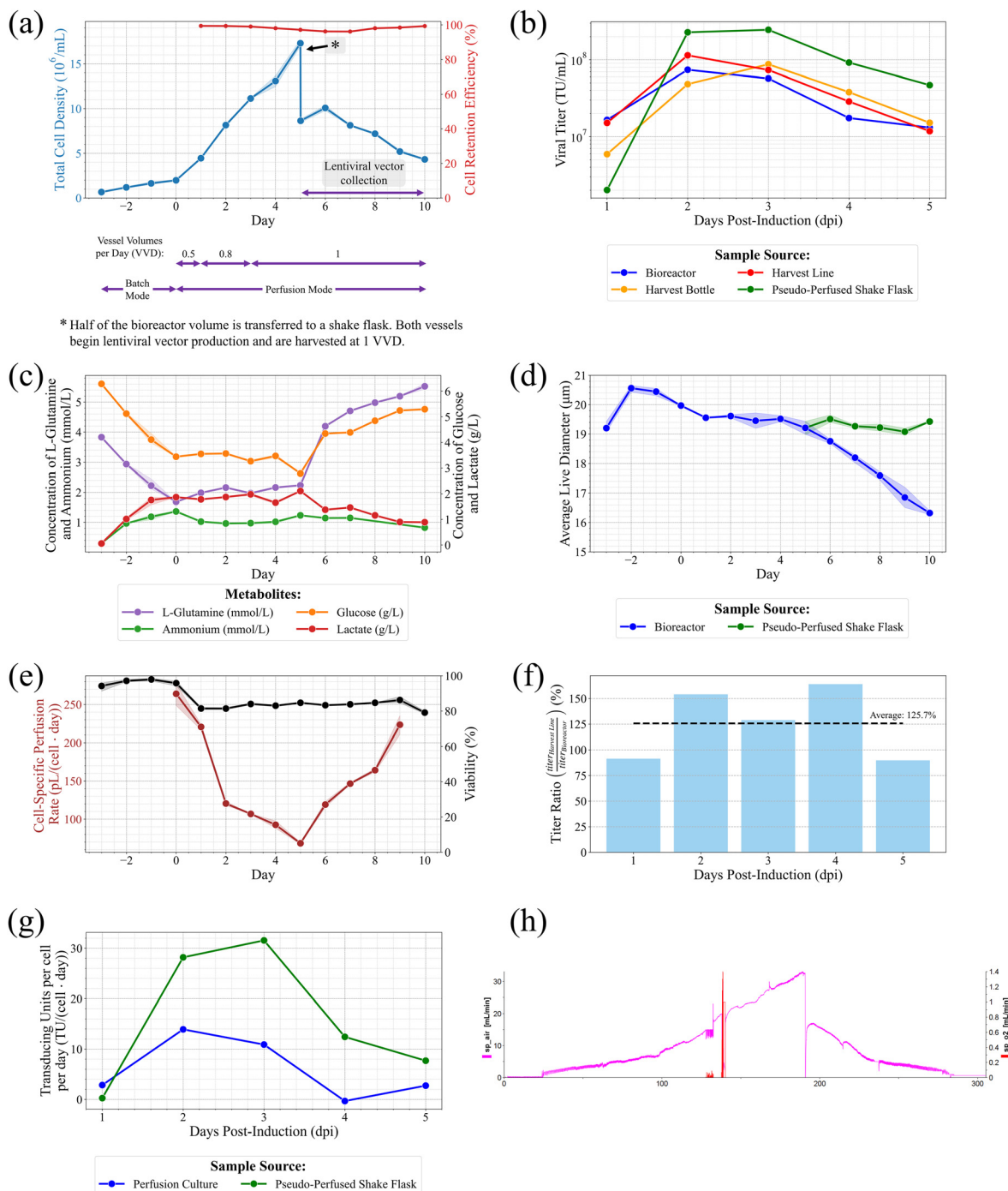


Fig. 3 Perfusion culture run 1. (a) Time-series data of the total cell density of HEK293 cells in the bioreactor and cell retention efficiency of the spiral microfluidic device. The plot is annotated with the vessel volumes per day (VVD) perfusion rate, whether the cultures are in perfusion mode or batch mode (by convention, days in batch mode are labeled as negative numbers), the time point when lentiviral vector production was initiated, and when samples were drawn and frozen at -80 °C to be titered later. Once the target cell density was achieved, half of the bioreactor volume was transferred to a shake flask, and both vessels were simultaneously induced, filled back to the working volume of 350 mL and then maintained at 1 VVD (as indicated by *). (b) Functional unconcentrated viral titer measurements at multiple sample sources during the lentiviral vector production phase. Functional titers (infectious particles) are in transducing units per mL (TU mL $^{-1}$) and are calculated using a Jurkat T cell infection assay. Bioreactor samples are taken from a syringe port attached to the main culture vessel; harvest line samples are taken directly from the fluid exiting the outward outlet; and harvest bottle samples are taken from the bottle where fluid from the outward outlet has accumulated over the past 24 hours. (c) Concentrations of L-glutamine, ammonium, glucose, and lactate in the bioreactor. (d) Average cell diameter in the bioreactor and the pseudo-perfused shake flask. (e) Cell-specific productivity and viability in the bioreactor. (f) Titer ratio, represented as the quotient of the functional titers measured in the harvest line and the bioreactor. (g) Cell-specific productivity (TU per cell per day) of the perfusion bioreactor and pseudo-perfused shake flask. Perfusion bioreactor: peak cell-specific productivity of 13.92 TU per cell per day at 2 dpi, cell-specific yield of 30.14 TU per cell. Pseudo-perfused shake flask: peak cell-specific productivity of 31.56 TU per cell per day at 2 dpi, cell-specific yield of 80.14 TU per cell. (h) Air and oxygen sparging rate to the bioreactor.



Table 1 Spiral device cell retention efficiency during four perfusion culture runs

| | Run 1 (10 days) | Run 2 (9 days) | Run 3 (11 days) | Run 4 (14 days) |
|-------------|-----------------|----------------|-----------------|-----------------|
| Mean (%) | 98.1 | 97.3 | 97.9 | 96.1 |
| Minimum (%) | 96.2 | 94.2 | 95.5 | 90.4 |

bioreactor had three distinct phases, shown in Fig. 3(c). First, during batch mode, without the addition of media *via* the media inlet or the removal of waste *via* the spiral device, the concentrations of L-glutamine and glucose lowered, and the concentrations of ammonium and lactate increased. During the cell growth phase, prior to induction, the VVD was controlled to maintain relatively stable metabolite concentrations. Once lentiviral vector production began, 1 VVD was maintained for consistency between the LV harvests of each run. One consequence of this was that L-glutamine and glucose levels were increased, whereas ammonium and lactate production were reduced, and those metabolites exited through the spiral device's outward outlet as waste. Average cell diameter remained stable in run 1 throughout the cell growth phase (Fig. 3(d)) but decreased during the LV production phase. Runs 2, 3, and 4 showed stable or slightly decreasing cell diameters prior to LV production, followed by sharp reductions in cell size after LV production began (Fig. S3(d)–S5(d)). In contrast, the average cell diameter of cells in the pseudo-perfused shake flask stayed the same pre- and post-induction, likely due to the gentler conditions. Another important parameter, the cell-specific perfusion rate (CSPR), was controlled to maintain constant nutrient and metabolite concentrations during the cell growth phase by adjusting the VVD as cell density increased (Fig. 3(e)). In all runs, the CSPR rose following the onset of LV production, since the high VVD was used exclusively to harvest LVs, not to promote cell growth. Cell viability dropped within the first day of perfusion mode as well, likely due to the higher shear experienced by cells in the spiral device compared with the bioreactor vessel. Once the cells are induced, they maintain roughly constant cell viability, with a precipitous drop in viability four days post-induction, which is more clearly seen in the longer harvests of runs 3 and 4 (Fig. S4(e) and S5(e)). Lastly, the air sparging rate over time follows a similar pattern to the bioreactor's cell density. Notably, in Fig. 3(h), once the cells are divided between the bioreactor and a pseudo-perfused shake flask and then induced at 192 hours post-inoculation, the cells commit to LV production and consume less oxygen.

3.3 Titer and cell-specific productivity comparison with shake flasks

Filtration membranes have a reputation for reducing product recovery over time due to the buildup of cell debris and cells on the membrane during a perfusion culture. Since spiral microfluidics does not rely on membranes, we expect product loss to be negligible. We also expect that the functional titers

taken each day from the bioreactor and the harvest line would be equal, since the spiral device does not inertially focus vector particles due to their smaller size relative to cells, and the outward outlet is large enough to expect a lossless harvest. The bioreactor and harvest line are reflective of the status of the perfusion culture (an instantaneous measurement at 37 °C), whereas measurements from the harvest bottle are time-averaged (past 24 hours).

During the seven-day continuous LV harvest from the 350 mL perfusion bioreactor in run 3 (Fig. S4(b)), 6.59×10^{10} TUs were recovered from the bioreactor, and the functional titers recorded in the bioreactor and the harvest line during this time are similar, suggesting that the spiral microfluidic cell retention device is capable of a high titer ratio over long continuous production periods. Previous studies researching antibody harvesting have given alternative names describing titer ratio, such as antibody recovery efficiency¹⁰ and product sieving.²³ In the former, they achieve an antibody recovery efficiency of approximately 100% and a total yield of 263 mg of IgG₁,¹⁰ suggesting a lossless recovery of valuable biopharmaceutical products from perfusion culture. Tran *et al.* report similar lentiviral vector functional titers between the perfusate and bioreactor samples with a TFDF-mediated perfusion culture.⁶

In Fig. S4(f), for run 3, the titer ratio is ~100% for 5 of the 7 days of collection, which suggests a sustained, lossless capture of LVs. On average, the titer ratio is 108.1% for this run. The other three perfusion cultures have run-averaged titer ratios of 125.7% (run 1, Fig. 3(f)), 122.7% (run 2, Fig. S3(f)), and 149.7% (run 4, Fig. S5(f)), which means on average, the titers measured in the harvest were higher than the corresponding titers measured in the bioreactor. While theoretically, it would follow that the titers in the bioreactor and harvest line should match, the slight favorability of LV ending up in the harvest may be due to shear-mediated release of infectious particles as cells travel through the spiral device. Still, these data suggest that the inertial microfluidic harvest of LVs has negligible loss.

Furthermore, the cell-specific productivities and yields of the perfusion cultures (and pseudo-perfused shake flasks if applicable) reveal the most relevant production periods, normalized by the total cell count. The maximum cell-specific productivities listed in Table 2 were all at 2 dpi. Consistent with the titers observed in the bioreactor and the pseudo-perfused shake flask, the cell-specific productivities and cell-specific yields are higher in the pseudo-perfused shake flask than in the bioreactor (Fig. 3(g)). Similar results were observed in run 2 (Fig. S3(g)).



Table 2 Maximum cell-specific productivities, cell-specific yields, and total yield of the top-performing runs

| | Perfusion bioreactor harvest | | | Pseudo-perfused shake flask | |
|--|------------------------------|-----------------------|-----------------------|-----------------------------|-----------------------|
| | Run 1 | Run 2 | Run 3 | Run 1 | Run 2 |
| Maximum cell-specific productivities (TU per cell per day) | 13.9 | 16.0 | 10.6 | 31.6 | 50.6 |
| Cell-specific yields (TU per cell) | 30.1 | 27.0 | 17.6 | 80.1 | 84.9 |
| Total yield (TU) | 7.28×10^{10} | 6.42×10^{10} | 6.59×10^{10} | 2.15×10^{11} | 2.62×10^{11} |

In Fig. 4, a comparison study was conducted to determine the relationship between initial cell density and vector output in 30 mL shake flasks. All cell cultures were in log-phase growth, and initial viable cell densities were artificially set by resuspending cultures of lower densities. Higher starting cell densities led to higher (3 dpi) functional titers (Fig. 4(a)). Additionally, when 3 dpi LV did not undergo a freeze/thaw cycle, the titers were even higher, exceeding 10^9 TU mL⁻¹ at the 15 M mL⁻¹ and 20 M mL⁻¹ starting viable cell densities. In practice, it is challenging in a manufacturing context to avoid LV freeze/thaw cycles, but the functional titers of samples collected at 3 dpi (no freeze/thaw) from this study are 1.72× to 4.85× higher than those of the 3 dpi LV samples that did undergo a freeze/thaw cycle. The cell-specific productivity (Fig. 4(b)) was highest with the '20 M mL⁻¹' starting condition at 24.52 TU per cell per day three days post-induction and an overall cell-specific yield of 34.2 TU per cell. As shown in Fig. 4(c), the cell densities observed match the pattern seen in the perfusion culture runs, where cell densities rise for one day (or two days at lower starting cell densities) and then fall during the most productive days.

Since runs 1 and 2 involved the division of bioreactor-cultured cells between the perfusion bioreactor and a pseudo-perfused shake flask, their viable cell density at the time of induction is closest to the '7.5 M mL⁻¹' shake flask condition of Fig. 4 and could be most closely benchmarked to that condition. As seen in Fig. 4(b), the cell-specific productivity of the 30 mL shake flask at 3 dpi is 8.44 TU per cell per day and the cell-specific yield is 10.64 TU per cell, which are outperformed by the perfusion bioreactor and pseudo-perfused shake flask conditions. When comparing runs 1 and 2 to the '20 M mL⁻¹' condition of Fig. 4, the pseudo-perfused shake flask condition outperforms, whereas the bioreactor condition does not.

3.4 Comparative benchmarking and scalability analysis

We compared the LV outputs we achieved with two other teams using inducible HEK293 producer cell lines for lentiviral vector generation with perfusion bioprocessing (Table 3). Here, we highlight run 2, which yielded the highest total functional particles: 2.62×10^{11} TU from the pseudo-perfused shake flask and 6.42×10^{10} TU from the bioreactor, for a combined total of 3.26×10^{11} TU. These results are comparable to the outcomes of run 1, which yielded 2.15×10^{11} TU from the pseudo-perfused shake flask and 7.28×10^{10} TU from the bioreactor, for a combined total of $2.88 \times$

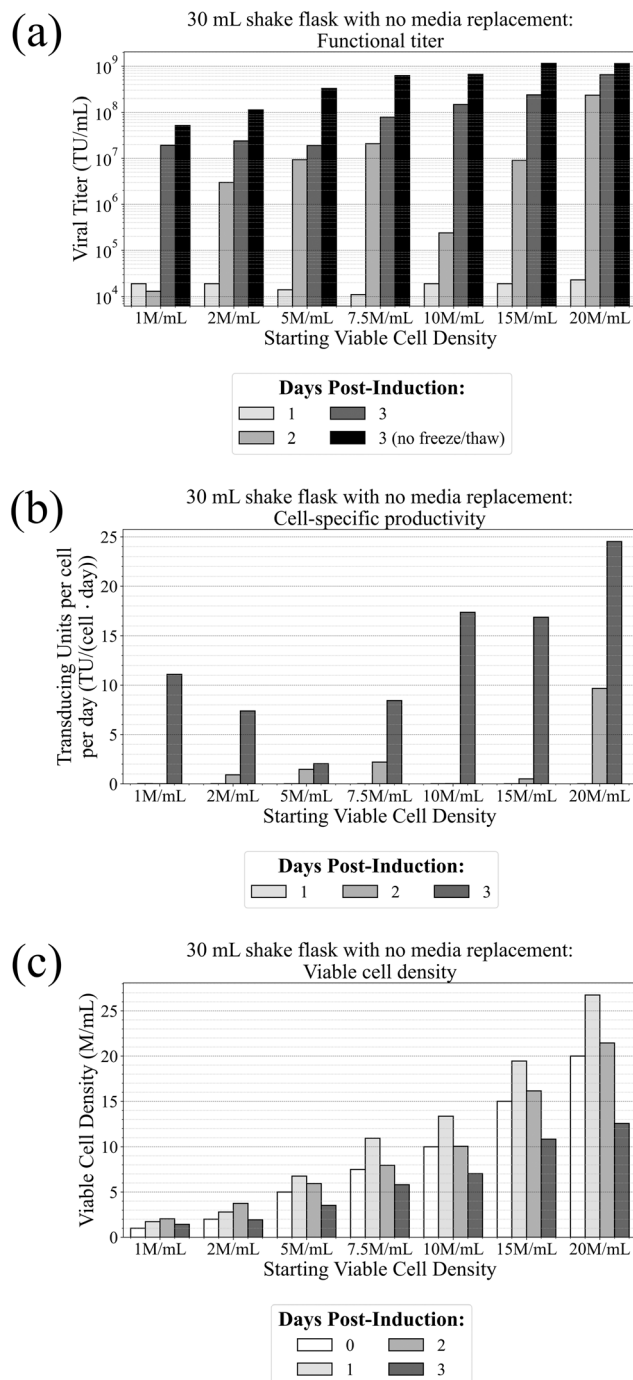


Fig. 4 Optimizing conditions for batch LV production. (a) Functional titer, (b) cell-specific productivity, and (c) viable cell density of 30 mL of HEK293 cells in shake flasks at different starting viable cell densities with no media replacement.



Table 3 Comparison of the process parameters from LV production in the perfusion bioreactor and the pseudo-perfused shake flask following cell growth in the perfusion bioreactor, and alongside the results of two other bioprocessing teams using inducible HEK293 producer cell lines generating LV encoding a GFP transgene

| Parameter | Run 2 (bioreactor) | Run 2 (pseudo-perfused shake flask) | Klimpel <i>et al.</i> , 2023 (ref. 1) | Tran and Kamen, 2022 (ref. 6) |
|--|-----------------------|---|---------------------------------------|----------------------------------|
| Bioreactor nominal volume (mL) | 500 | — | 5000 | 3000 |
| Bioreactor working volume (mL) | 350 | 350 | 4500 | 2000 |
| Cell retention device | Spiral microfluidics | — | Acoustic wave separation | Tangential flow depth filtration |
| Transgene | GFP | GFP | WAS-T2A-GFP | GFP |
| Total functional particles harvested (TU) | 6.42×10^{10} | 2.62×10^{11} | 6.36×10^{11} | 3.9×10^{11} |
| TU _{total} mL _{bioreactor} ⁻¹ | 1.83×10^8 | 7.49×10^8 | 1.41×10^8 | 1.95×10^8 |
| Maximum TU mL ⁻¹ | 7.06×10^7 | 4.42×10^8 | 2.41×10^7 | 1.2×10^8 |
| Maximum TU per cell per day | 16.03 | 50.55 | 1.48 | 7 |
| Vector generation time (hours) | 72 | 72 | 234 | 96 |
| Total culture time (hours) | 288 | 288 | 299 | 288 |
| Inoculation density (M mL ⁻¹) | 0.35 | Originates from run 2 bioreactor | 1 | 0.35 |

10^{11} TU. To take into consideration the different bioreactor sizes, we normalized total production by the working volume of the bioreactor, and our results are competitive with other teams that are using traditional cell retention devices. Additionally, the processes were all approximately the same length (288 to 299 hours).

The total TU generated per mL of working volume in the bioreactor (TU_{total} mL_{bioreactor}⁻¹) in run 2 is comparable to the results achieved with the acoustic wave separation¹ and tangential flow depth filtration devices.⁶ Furthermore, the cells in the pseudo-perfused shake flask, which originated from the spiral device-perfused bioreactor, produced an even higher total TUs per mL of the flask's working volume (TU_{total} mL_{bioreactor}⁻¹). The cell-specific productivity and yields from runs 1 and 2's pseudo-perfused shake flasks are exceptionally high, likely due to cell line selection, the simplicity of the GFP transgene compared to therapeutically relevant transgenes, the upstream production strategy, and the relatively lossless downstream processing prior to the transduction of Jurkat cells. The bioreactor's maximum cell-specific productivity of 16.03 TU per cell per day at 2 dpi and cell-specific yield of 27.0 TU per cell (Fig. S3(g)) are also competitive with published production processes.

Additionally, we used SFCA filters to process all our samples identically, but a different filter material may have been more advantageous. For example, harvest bottle samples from run 1 filtered through 0.45 μm polyvinylidene difluoride (PVDF) filters (Millipore, USA) had functional titers that were 1.14× to 2.01× higher than their SFCA-filtered counterparts. This suggests that the titers reported in this work could be even higher with a filter material optimized for this downstream process.

LV production by cells transferred from the bioreactor to the pseudo-perfused shake flask was higher than production by cells remaining in the bioreactor. This is most likely described by differences in shear exposure between the two production environments. The Reynolds numbers in the stirred-tank bioreactor (ranging from 9338 to 13 163) and pseudo-perfused

shake flask (77569) are both representative of the turbulent hydrodynamic regime. Giese *et al.* determined that shear rates in 50 mL to 1000 mL shake flasks range from 20 s⁻¹ to 2000 s⁻¹, with shear rates rising with higher orbital rotation speeds, larger flask volumes, and smaller filling volumes.²⁴ We calculated an effective shear rate of 127 s⁻¹ to 213 s⁻¹ in the perfusion bioreactor, using scaling relationships and constants adapted from the relevant literature.^{22,24,25} Based on comparisons with Giese *et al.*'s work,²⁴ for our culture conditions, we expect the pseudo-perfused shake flask's effective shear rate to be on the same order of magnitude as the perfusion bioreactor. The particle tracing simulation for the spiral cell retention device (Fig. S7(c)) estimates a 0.6 second residence time of cells with each pass through the device. We computed an effective shear rate of 8642 s⁻¹ through the device, which is higher than the 4000 s⁻¹ to 6000 s⁻¹ shear rates observed with TDFD operation.²⁶ Since the bioreactor's operating volume is 350 mL and the inlet flow rate is 6 mL min⁻¹, the entire bioreactor's operating volume, on average, is transited through the spiral microfluidic device once every 58.3 minutes, even though the period of high shear exposure is brief. Since the shear rates between the two vessels are within the same order of magnitude, and the shear rate within the spiral device is significantly higher, it is likely that the elevated shear rate from the spiral device on cells during lentiviral vector production is not the optimal choice among the options investigated, although its performance metrics are still competitive with existing strategies in Table 3. A stability study conducted by Perry *et al.* shows that lentiviral vectors are stable up to shear rates of at least 10⁵ s⁻¹ while maintaining stable functional titers,²⁷ which is 11.5× higher than the effective shear rate we report. This suggests that the cells, rather than the lentiviral vectors, are mainly affected by the elevated shear rates. The calculations for all Reynolds numbers and shear rate values reported can be found in the SI.

The PDMS spiral microfluidic devices used to conduct this work are relatively inexpensive to produce (<\$5), especially



compared to conventional cell retention technologies. The studies highlighted in Table 3 were completed with stable producer cell lines. Teams producing lentiviral vectors generated by triple transfection in suspension-adapted HEK293T cell culture also have functional titers on the order of 10^7 to 10^8 TU mL⁻¹.^{28,29} In one study, a one-liter batch production led to titers ranging from 8.2×10^7 TU mL⁻¹ to 3.7×10^8 TU mL⁻¹ two days post-transfection,²⁸ while in a different study with a larger working volume of 5.5 L, the reported titer was 1.5×10^7 TU mL⁻¹ four days post-transfection.²⁹ These titer values will vary depending on the specific cell line, the plasmids used, the transfection efficiency, and the process scale.

Filtration-based cell retention devices scale to various bioreactor sizes by increasing membrane surface area, and this is supported by an extensive ecosystem of commercially available, validated products. In contrast, this study described the use of a single spiral device accepting an input flow rate of 6 mL min⁻¹ with a harvest stream of 0.12 mL min⁻¹ to 0.24 mL min⁻¹, depending on the perfusion rate. Scaling this technology to larger bioreactors would rely on spiral device parallelization, where multiple plastic spiral microfluidic devices are stacked on top of one another to divide an input flow rate across many layers,¹³ resulting in a flow rate of 6 mL min⁻¹ per spiral. For example, to use 20 spirals in a cell retention device, the input flow rate would be 120 mL min⁻¹, and the harvest flow rate would range from 2.4 mL min⁻¹ to 4.8 mL min⁻¹, depending on the perfusion rate. With sufficiently large-diameter tubing attached to the inlet and outlet ports of the device, we would expect comparable shear rates for the cells as they travel through either the PDMS spiral device or the stackable plastic spiral device. In this work, we sterilized the perfusion culture assembly as a closed system with the spiral device attached, whereas with a stackable plastic spiral microfluidic device, the unit would need to be gamma-irradiated for sterilization and the remainder of the assembly autoclaved separately.

4. Conclusion

Using a PDMS spiral microfluidic cell retention device, we were able to achieve cell densities between 15×10^6 and 25×10^6 cells per mL and induce the cells to generate lentiviral vectors to achieve an estimated recovered, unconcentrated, functional LV yield on the order of 10^{10} TU per 350 mL bioreactor vessel, with peak productivities typically occurring two days post-induction and reaching functional titers on the order of 10^8 TU mL⁻¹. On average, the spiral device maintained >97% cell retention efficiency during these perfusion cultures. When cells are cultivated in the perfusion bioreactor and divided evenly between the bioreactor at 1 VVD and a pseudo-perfused shake flask with daily media replacement (effectively, 1 VVD as well), the pseudo-perfused shake flask's titers outperformed those of the bioreactor (yielding 10^{11} TU per 350 mL shake flask). The titer ratio of the spiral device was, on average, above 1, suggesting slight favorability of the lentiviral vectors to travel through the outward outlet of the spiral device, and therefore lead to a lossless recovery of vectors that is competitive with

other bioprocessing teams. Our top three bioreactor runs achieved cell-specific yields of 17.6 to 30.1 TU per cell, and the two pseudo-perfused shake flasks achieved over 80 TU per cell.

Author contributions

Alexander Bevacqua: conceptualization, formal analysis, investigation, methodology, validation, visualization, writing – original draft, writing – review & editing. Fuguo Liu: investigation, methodology, writing – review & editing. Jianzhu Chen: conceptualization, funding acquisition, project administration, resources, supervision, writing – review & editing. Jongyoon Han: conceptualization, funding acquisition, project administration, resources, supervision, writing – review & editing.

Conflicts of interest

There are no conflicts of interest to declare.

Data availability

The data supporting this article have been included as part of the supplementary information (SI).

Supplementary information is available. See DOI: <https://doi.org/10.1039/d6lc00029k>.

Acknowledgements

The authors thank Dr. Aziza P. Manceur of the National Research Council Canada for the HEK293 producer cell line and helpful discussions related to the cell line. This work was financially supported by the National Science Foundation Graduate Research Fellowship Program under Grant 2141064 and the US Food and Drug Administration under Grant 1R01FD007480-03. Any opinions, findings, and conclusions or recommendations expressed in this material are those of the authors and do not necessarily reflect the views of the National Science Foundation or the US Food and Drug Administration. The authors also thank the Massachusetts Institute of Technology Koch Institute's Robert A. Swanson (1969) Biotechnology Center for technical support, specifically the Flow Cytometry Core (RRID:SCR_017892), which is supported in part by the Koch Institute Support (core) Grant P30-CA014051 from the National Cancer Institute.

References

- 1 M. Klimpel, M. Terrao, N. Ching, V. Climenti, T. Noll, V. Pirzas and H. Laux, *Biotechnol. Bioeng.*, 2023, **120**, 2622–2638.
- 2 R. M. Comisel, B. Kara, F. H. Fiesser and S. S. Farid, *Biochem. Eng. J.*, 2021, **167**, 107868.
- 3 R. M. Tona, R. Shah, K. Middaugh, J. Steve, J. Marques, B. R. Roszell and C. Jung, *Mol. Ther.–Methods Clin. Dev.*, 2023, **29**, 93–107.
- 4 A. P. Manceur, H. Kim, V. Mistic, N. Andreev, J. Dorion-Thibaudeau, S. Lanthier, A. Bernier, S. Tremblay, A. M.



- Gélinas, S. Broussau, R. Gilbert and S. Ansoerge, *Hum. Gene Ther: Methods*, 2017, **28**, 330–339.
- 5 M. Klimpel, B. Pflüger-Müller, M. A. Cascallana, S. Schwingal, N. I. Lal, T. Noll, V. Pirzas and H. Laux, *Biotechnol. Bioeng.*, 2024, **122**, 344.
 - 6 M. Y. Tran and A. A. Kamen, *Front. Bioeng. Biotechnol.*, 2022, **10**, 1024.
 - 7 S. Broussau, V. Lytyn, M. Simoneau, C. Guilbault, M. Leclerc, N. Nazemi-Moghaddam, N. Coulombe, S. M. Elahi, S. McComb and R. Gilbert, *Mol. Ther.–Methods Clin. Dev.*, 2023, **29**, 40–57.
 - 8 D. J. Stibbs, P. Silva Couto, Y. Takeuchi, Q. A. Rafiq, N. B. Jackson and A. C. M. E. Rayat, *Mol. Ther.–Methods Clin. Dev.*, 2024, **32**, 1–11.
 - 9 S. Ansoerge, O. Henry and A. Kamen, *Biochem. Eng. J.*, 2010, **48**, 362–377.
 - 10 T. Kwon, H. Prentice, J. De Oliveira, N. Madziva, M. E. Warkiani, J. F. P. Hamel and J. Han, *Sci. Rep.*, 2017, **7**, 1–11.
 - 11 M. Mayani, S. Nellimarla, R. Mangalathillam, H. Rao, S. Patarroyo-White, J. Ma and B. Figueroa, *Biotechnol. Prog.*, 2023, 1–12.
 - 12 M. E. Warkiani, A. K. P. Tay, G. Guan and J. Han, *Sci. Rep.*, 2015, **5**, 1–10.
 - 13 H. Jeon, T. Kwon, J. Yoon and J. Han, *Lab Chip*, 2022, **22**, 272–285.
 - 14 J. Schellenberg, M. Dehne, F. Lange, T. Scheper, D. Solle and J. Bahnemann, *Bioengineering*, 2023, **10**, 656.
 - 15 T. Kwon, R. Yao, J. F. P. Hamel and J. Han, *Lab Chip*, 2018, **18**, 2826–2837.
 - 16 C. Perry and A. C. M. E. Rayat, *Viruses*, 2021, **13**, 1–46.
 - 17 M. Soldi, L. Sergi Sergi, G. Unali, T. Kerzel, I. Cuccovillo, P. Capasso, A. Annoni, M. Biffi, P. M. V. Rancoita, A. Cantore, A. Lombardo, L. Naldini, M. L. Squadrito and A. Kajaste-Rudnitski, *Mol. Ther.–Methods Clin. Dev.*, 2020, **19**, 411–425.
 - 18 A. P. Cribbs, A. Kennedy, B. Gregory and F. M. Brennan, *BMC Biotechnol.*, 2013, **13**, 98.
 - 19 B. L. Ellis, P. R. Potts and M. H. Porteus, *Hum. Gene Ther.*, 2011, **22**, 93.
 - 20 K. H. D. Crawford, R. Eguia, A. S. Dingens, A. N. Loes, K. D. Malone, C. R. Wolf, H. Y. Chu, M. A. Tortorici, D. Veessler, M. Murphy, D. Pettie, N. P. King, A. B. Balazs and J. D. Bloom, *Viruses*, 2020, **12**, 513.
 - 21 J. Coronel, C. Heinrich, S. Klausing, T. Noll, A. Figueredo-Cardero and L. R. Castilho, *Biotechnol. Prog.*, 2020, **36**, e2915.
 - 22 C. Dinter, A. Gumprecht, M. A. Menze, A. Azizan, P. J. Niehoff, S. Hansen and J. Büchs, *Sci. Rep.*, 2024, **14**, 3658.
 - 23 D. WuDunn, A. Squeri, J. Vu, A. Dhingra, J. Coffman and K. Lee, *Biotechnol. Prog.*, 2024, **40**, e3440.
 - 24 H. Giese, W. Klöckner, C. Peña, E. Galindo, S. Lotter, K. Wetzel, L. Meissner, C. P. Peter and J. Büchs, *Chem. Eng. Sci.*, 2014, **118**, 102–113.
 - 25 R. R. Hemrajani and G. B. Tatterson, in *Handbook of Industrial Mixing: Science and Practice*, ed. E. L. Paul, V. A. Atiemo-Obeng and S. M. Kresta, John Wiley & Sons, Inc., Hoboken, New Jersey, 2004, pp. 345–390.
 - 26 J. P. Mendes, B. Fernandes, E. Pineda, S. Kudugunti, M. Bransby, R. Gantier, C. Peixoto, P. M. Alves, A. Roldão and R. J. S. Silva, *Front. Bioeng. Biotechnol.*, 2022, **10**, 1020174.
 - 27 C. Perry, N. Mujahid, Y. Takeuchi and A. C. M. E. Rayat, *Biotechnol. Bioeng.*, 2024, **121**, 2466–2481.
 - 28 M. Bauler, J. K. Roberts, C. C. Wu, B. Fan, F. Ferrara, B. H. Yip, S. Diao, Y. I. Kim, J. Moore, S. Zhou, M. M. Wielgosz, B. Ryu and R. E. Throm, *Mol. Ther.–Methods Clin. Dev.*, 2020, **17**, 58–68.
 - 29 Q. L. Tang, L. X. Gu, Y. Xu, X. H. Liao, Y. Zhou and T. C. Zhang, *Bioengineered*, 2021, **12**, 2095–2105.

